(1)

COMPONENT PART NOTICE

THIS PAPER IS A COMPONENT PART OF THE FOLLOWING COMPILATION REPORT:

TITLE: Proceedings of the Antenna Applications Symposium Held in Urbana, Illinois on 17-19 September 1986. Volume 1.

TO ORDER THE COMPLETE COMPILATION REPORT, USE AD-A181 536.

THE COMPONENT PART IS PROVIDED HERE TO ALLOW USERS ACCESS TO INDIVIDUALLY AUTHORED SECTIONS OF PROCEEDING, ANNALS, SYMPOSIA, ETC. HOWEVER, THE COMPONENT SHOULD BE CONSIDERED WITHIN THE CONTEXT OF THE OVERALL COMPILATION REPORT AND NOT AS A STAND-ALONE TECHNICAL REPORT.

THE FOLLOWING COMPONENT PART NUMBERS COMPRISE THE COMPILATION REPORT:

AD#: P005 394 thru P005 409 AD#:

AD#: AD#:

AD#: AD#:

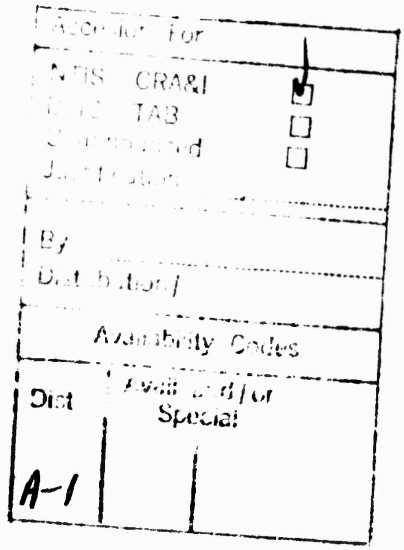

EHF/SHF SATCOM ANTENNA AND RADOME TEST RESULTS

Allen L. Johnson
Wayne O. Fischbach
Avionics Laboratory
Wright-Patterson AFB, Ohio 45433

ABSTRACT

The current airborne EHF SATCOM system has a RF power output of 100 watts and an antenna beamwidth of less than 1 degree. As the RF beam from the antenna passes through the dielectric radome it will be refracted at each surface. The resulting change in direction of the beam depends on the frequency, the dielectric constant of the radome, and the shape of the radome surfaces. Tests have been performed to evaluate the beam deflection at 20 and 44 Giga-Hertz. Other systems effects which were evaluated included antenna beam distortion, RF heating, and Radio Frequency Interference between two antennas (SHF and EHF) under a single radome.

INTRODUCTION

Command post aircraft currently use satellite communications (SATCOM) to achieve worldwide connectivity. Early SATCOM systems employed the Ultra High Frequency (UHF) band, with simple aerodynamic blade or overhead-looking antennas (Armstrong, 1978). As the communications systems became more sophisticated, the use of the microwave frequency bands became practical. Antennas now used for SATCOM include Super High Frequency (SHF) and Extremely High

Frequency (EHF) dishes, (Schultz, 1983). These antennas must be placed under radomes to maintain the aerodynamics of the airborne command post. The Avionics Laboratory has investigated the effects of narrow-beam systems since it undertook the development of its first microwave SATCOM system in 1969. We are currently flight testing our fifth generation microwave SATCOM system, (Joyner, 1981).

Some of the operational command post aircraft are already equipped with SHF SATCOM systems to allow operation with the 7-8 Gigallertz (GHz) Defense Satellite Communications System (DSCS II & DSCS III). With the advent of the MILSTAR system, which operates at 20 and 44 GHz, these command post aircraft will require a radome capable of handling 7/8, 20, and 44 GHz: i.e. a tri-band radome.

A tri-band radome has been developed for the Avionics Laboratory's SATCOM system aboard the C-135 testbed aircraft which is maintained and operated by the 4950th Test Wing, (Joyner, 1985). Evaluation of the parameters and effects of the C-135 radome is necessary to validate models used to predict the radome characteristics and reduce the risk associated with future tri-band radome developments.

AN/ASC-30 SATCOM SYSTEM TESTS

The AN/ASC-30 EHF SATCOM system has a Radio Frequency (RF) power output of 100 watts and an antenna beamwidth of less than 1 degree. As the RF beam from the antenna passes through the

dielectric radome it is refracted at each surface. The resulting change in direction of the beam, called beam squint, depends on the frequency, the dielectric constant of the radome, and the shape of the radome surfaces. Tests have been performed to evaluate the beam squint at 20 and 44 GHz.

Other systems effects which were evaluated included radome attenuation, antenna beam shape, RF heating, Radio Frequency Interference (RFI) between two antennas under a single radome, and radome deflection in flight.

RF Beam Squint

Measurements of the RF beam squint were accomplished by comparing the optimum antenna pointing angles with the radome in place and removed. One practical problem in measuring the beam squint of the AN/ASC-30 tri-band radome was the lack of a 20/44 GHz satellite on-orbit to use as a signal source. In place of the satellite, a simulator was used, consisting of a 20 GHz transmitter and a 44 GHz receiver on the tower of building 620 at WPAFB, OH, Figure 1. The AN/ASC-30 with its 44 GHz transmitter and 20 GHz receiver was installed in aircraft C-135/372, which was located on the ground at Patterson Field.

For the beam squint test the 20 GHz tower transmitter and 44 GHz aircraft transmitter were turned on and their antennas pointed toward the respective receivers. The aircraft antenna was moved in 0.1° azimuth steps for ±2.5°, and 0.1° elevation steps for ±1.0° of

the calculated pointing angle from the aircraft to the tower. In the tower and aircraft, the azimuth antenna beam patterns were received, recorded, and correlated with the transmitter pointing angles. The radome was then removed and the azimuth/elevation steps repeated. Any difference in the pointing angle for the peak of the beam was attributed to radome-induced beam squint. Due to the complex curvature of the radome, various portions were measured from the nose, to broadside, to the tail, Figure 2.

Radome Attenuation

It was possible to measure the absolute attenuation of the radome at 20 and 44 GHz by comparing the received power with and without the radome in the line-of-sight path, using the same test configuration as for beam squint.

Antenna Beam Shape

The pattern of AN/ASC-30 EHF antenna is also of interest. The beam squint measurements provided the information necessary to characterize the affect of the radome and ribs on the three-dimensional beam shape.

Radome RF Heating

When an SHF transmitted beam passes through the radome, local RF heating will occur. For the RF heating tests a special test fixture was constructed to simulate a section of the C-135 aircraft fuselage. The AN/ASC-18 airborne SATCOM antenna was mounted on the fixture and the tri-band radome installed over the antenna,

Figure 3. The AN/ASC-18 terminal, which was installed in the nearby Rooftop Facility, has a power output of 10 kW in the SHF band. To conduct the test, the SHF transmitter was turned on and operated until the radome's inside temperature stabilizes. The extent of the heating was measured by attaching a series of heat tabs (which blacken at a specific temperature) around a 15 inch diameter circle inside the radome in the area where the antenna beam intercepted the radome. The test procedures require the SHF transmit power to be raised from a 2 kW level to a maximum of 10 kW in four steps. At a 10 kW transmit power level, the uniform energy density from the antenna would be 12.4 watts/inch^2. In the near field, the energy distribution is not uniform and it was anticipated that "hot spots" could occur with energy densities of 20 watts/inch^2. Tests with flat panels of the radome material indicated that at 8 GHz the loss in the radome is approximately 2dB (60% transmission). In a hot spot it was expected that 8 watts/inch^2 could be dissipated in the radome skin. The maximum temperature was determined for each power level by reading the highest temperature heat tab which had fired (blackened).

RFI/EMI Between Two Antennas Under One Radome

For some airborne command post applications, two dish antennas will be mounted under the same radome. One antenna system operates at 7 and 8 GHz while the other operates at 20 and 44 GHz. For the RFI/EMI test, the 20 GHz noise out of the 8 GHz transmitter that

couples into the 20 GHz antenna/receiver and the 7 GHz noise from the 44 GHz transmitter that couples into the 7 GHz antenna/receiver were measured. Both antennas were mounted on the test fixture, under the tri-band radome. Receiver measurements were made as each transmitter was turned on. The antennas were positioned at various geometrics; both pointed toward the same equal-angle reflection point, both antennas normal to the radome wall, and the antennas pointed almost directly toward each other.

Radome Deflection In Flight

The AN/ASC-30 system employs a 26" parabolic antenna that is mounted on top of a C-135 test aircraft. An aerodynamic radome covers the antenna to reduce the drag, Figure 4. Since the radome has to pass three frequency bands (7-8 GHz, 20-21 GHz, and 43-45 GHz), a special wall thickness design was required. The resulting thin-wall radome design did not have sufficient stiffness to meet deflection limits during maximum aerodynamic loading. To improve the stiffness, three ribs were added to the radome, Figure 5. The final design was run on a NASTRAN computer model (WANG, 1984) to calculate the radome wall deflection during an 8° aircraft sideslip, the maneuver specified as providing the maximum dynamic loading to the sides of the radome.

The tri-band radome was constructed by Hitco Inc. under a subcontract with Bell Aerospace Corp. and the Raytheon Company. The radome was then installed on the C-135/372 test aircraft and a

test flown to measure the actual deflection (Hocutt, 1985).

The tri-band radome was modelled by Bell Aerospace Corp. using a NASTRAN finite element computer model. The radome surface was divided into 320 separate panels and pressure levels calculated for the specific maneuver were applied to each panel. After several iterations of different skin thickness and rib placement, a final design was achieved with a skin thickness of 0.145 inches and rib placement shown in Figure 6. The maximum deflection location and value were predicted to be 0.251 inches at node 1056 with the 8° sideslip maneuver, Figure 7.

To measure radome deflection, a fixture was constructed by the 4950th TW to fit over the AN/ASC-30 antenna, Figure 8. Two linear deflection transducers were mounted at the edges of the fixture and the deflection arm attached to buttons cemented to the insides of the radome. The buttons were positioned within a few inches of the predicted maximum deflection point. The linear deflection transducers were connected to a DC power source and to the instrumentation system. The transducers had a travel of ±1.5 inches from their static position. The transducer position was calibrated over the entire travel range and recorded on a magnetic recorder and a chart recorder to an accuracy of 0.001 inches.

TEST RESULTS

Radome Beam Squint Measurements

A comparison of the antenna azimuth angle with the AN/ASC-30 tri-band radome both in place and removed provided a measurement of

the beam squint. A summary of the beam squint for various portions of the radome (azimuth angles) is shown in Figure 9. One azimuth sweep showing the worst beam squint is presented in Figure 10. The beam squint appears to be approximately 0.4° over the nose and tail and on the order of 0.1° broadside.

Radome Attenuation Measurements

In an effort to evaluate the effect of radome thickness and incidence angles on the radome attenuation, a 36-inch square flat panel was constructed of the same material and thickness as the tri-band radome. Attenuation tests were conducted on the flat panel. The results of the 20 GHz and 44 GHz measurements are shown in Figure 11.

Measurements of the actual radome attenuation were made by comparing the received signal level with the AN/ASC-30 tri-band radome in place and removed. A plot of the attenuation for various portions of the radome is shown in Figure 12. The radome attenuation measurements are in close agreement with the flat panel measurements.

Antenna Pattern

The 44 GHz pattern of the tri-band antenna was measured with the radome in place and removed. The mainbeam portion of the pattern is shown as a 3 dimensional plot, Figure 13. This data shows the effects of the radome and ribs particularly on the sidelobe distribution.

Radome Heating

The AN/ASC-18 SHF transmitter was first operated at 2 kW RF power at 8 GHz. The ambient temperature was approximately 40°F outside the radome and 50°F inside the radome. After 20 minutes of operation, the radome temperature stabilized at less than 100°F at the top and left side of the test circle, 105°F at the right side, and 115°F at the bottom. Following each power level setting, the maximum temperatures were recorded, Table 1.

TABLE 1 Temperature Distribution On Tri-Band Radome

Xmit Power	Measurement	0°	90°	180°	270°	Time
2 KW	Temp Tabs Thermocouple	100°F	105°F	115°F	100°F	20 Min
5 KW	Temp Tabs Thermocouple	100° 100°	115° 100°	130° 125°	100° 100°	15 Min
8 KW	Temp Tabs Thermocouple	130° 135°	130° 170°	130° 180°	130° 135°	32 Min
10 KW	Temp Tabs Thermocouple	130° 176°	130° 180°	200° 188°	130° 176°	16 Min

With the transmitter operating at 5 kW of power for 15 minutes, the maximum temperature recorded was 130°F. After transmitting 8 kW for 32 minutes, the temperature tabs on the bottom of the circle showed 130° but a thermocouple measured 180°F. The maximum power transmitted was 10 kW for 16 minutes, after which the temperature tabs showed 200°F at the bottom of the circle. Subsequent discoloring of the radome material indicated that the

internal plys of the radome reached a temperature of approximately 500° F during the 10 kW run.

From the measurements, it appears that the current tri-band radome design could withstand between 2 and 5 kW of transmit power at 8 GHz without experiencing an excessive temperature rise. Power levels above 5 kW are likely to cause an excessive temperature build up in the laminated plys which could damage the radome. If the radome loss were reduced, the transmit power could be increased proportionally.

RFI/EMI Test

With the AN/ASC-18 transmitting at 8.0 GHz, the AN/ASC-30 system encountered no interference at 20.8 GHz except when the transmit antenna was pointed at 225° azimuth where the mainbeam just grazed the AN/ASC-30 antenna. In that configuration, the worst case interference was with the AN/ASC-30 pointing at 180° azimuth and 80° elevation. Approximately a 1 dB rise was noticed in the noise floor of the AN/ASC-30 receiver when the AN/ASC18 was transmitting 10 kW. It was postulated that the interference was caused by energy coupling directly into the RF mixer and downconverter that is mounted on the back of the dish, rather than through the antenna feed. The RF mixer and downconverter were removed, reinstalled, and all connectors properly tightened. A retest showed only 0.1 dB rise in the noise floor. To determine the effect of the interference on link performance, data was

transmitted to the AN/ASC-30 system with the interference source on and off. The Bit Error Rate (BER) performance of the system appeared to be uneffected by the interference, Figure 14.

When the AN/ASC-30 transmitted 100 watts at 44 GHz, no interference was experienced in the AN/ASC-18's 7 GHz receive system, regardless of the orientation of the two antennas.

Radome Deflection Flight Test

During the aircraft's take-off roll, at a speed of approximately 90 knots, both sides of the radome started to deflect outward, Figures 15. As the aircraft reached take-off speed, rotated, and continued to accelerate, both sides of the radome deflected outward approximately 0.09 inches. The aircraft climbed to an altitude of 10,000 feet and the outward deflection remained constant during straight and level flight. The aircraft made a data run at 200 Knots Indicated Air Speed (KIAS) with a 5° side slip. There was no noticeable change in the radome deflection. Several runs were made at 10,000 feet altitude, 200 KIAS, with an 8° side slip. The instrumentation recorded a deflection of one minor division (approximately 0.04 inches) inward on both sides of the radome during those runs, Figure 16.

During the aircraft's approach and landing the radome deflection decreased on both sides as the airspeed decreased, Figure 17. Shortly after touch-down the instrumentation showed the radome had returned to its static width.

It appears the aerodynamic pressure on the front and top of the radome causes both sides to bow outward approximately 0.10 inches at the antenna station. The effect of the side-slip maneuver appears to reduce the front and top pressures, allowing both sides of the radome to move inward 0.04 inches. The effect of the dynamic pressure on the sides of the radome appears to be so small that it is masked by the change in front and top pressures.

The NASTRAN model which predicted an inward deflection of 0.25 inches during the side slip appears to be quite conservative. The model was used previously to predict the deflection on a dual-band radome (Severyn, 1978). A similar flight test of the dual-band radome produced deflections which agreed quite closely with the model (Cummins, 1978). The difference between the tri-band radome prediction and the test results may be due to inaccurate pressure distributions in the model or to the difficulty of correctly modeling the stiffness of the ribs.

REFERENCES

Armstrong, E.L., Maj (USAF), "AFSATCOM," Air Force Magazine, pp 80-85, July 1978.

Cummins, W.S., "Airworthiness Test of Dual Frequency SATCOM Radome," 4950th TW, Wright-Patterson AFB, OH, 2 June 1978.

Hocutt, Capt A.M., "Tri-band Radome Test Plan," AFWAL TM-85-13, Air Force Wright Aeronautical Laboratories, Wright-Patterson AFB, OH, 27 June 1985.

Johnson, A.L., "Airborne EHF Satellite Communications Terminals," Submitted to IEE Proceedings F, Herts England, July 1985.

Joyner, T.E., "AN/ASC-30 EHF/SHF Command Post SATCOM Terminal," NAECON Symposium, Vol 1, pp 124-127, Dayton OH, 19 May 1981.

Joyner, T.E., "AN/ASC-30 Upgrade SATCOM Moderate Gain Antenna/ Radome Subsystem," NAECON Symposium, pp 1192-1197, Dayton OH, 20 May 1985.

Schultz,J.B., "MILSTAR To Close Dangerous C^3I Gap," Defence Electronics, Vol 15 No. 3, pp 46-59, March 1983.

Severyn, T., "Aerodynamic Evaluation of Dual Frequency Radome," Flight Test Plan 78-4-3, 4950th TW, Wright-Patterson AFB, OH, 5 May 1978.

Wang, T., "AN/ASC-30 Upgrade Radome Structural Analysis," Bell Aerospace Corp, Buffalo, NY, 13 December 1984.

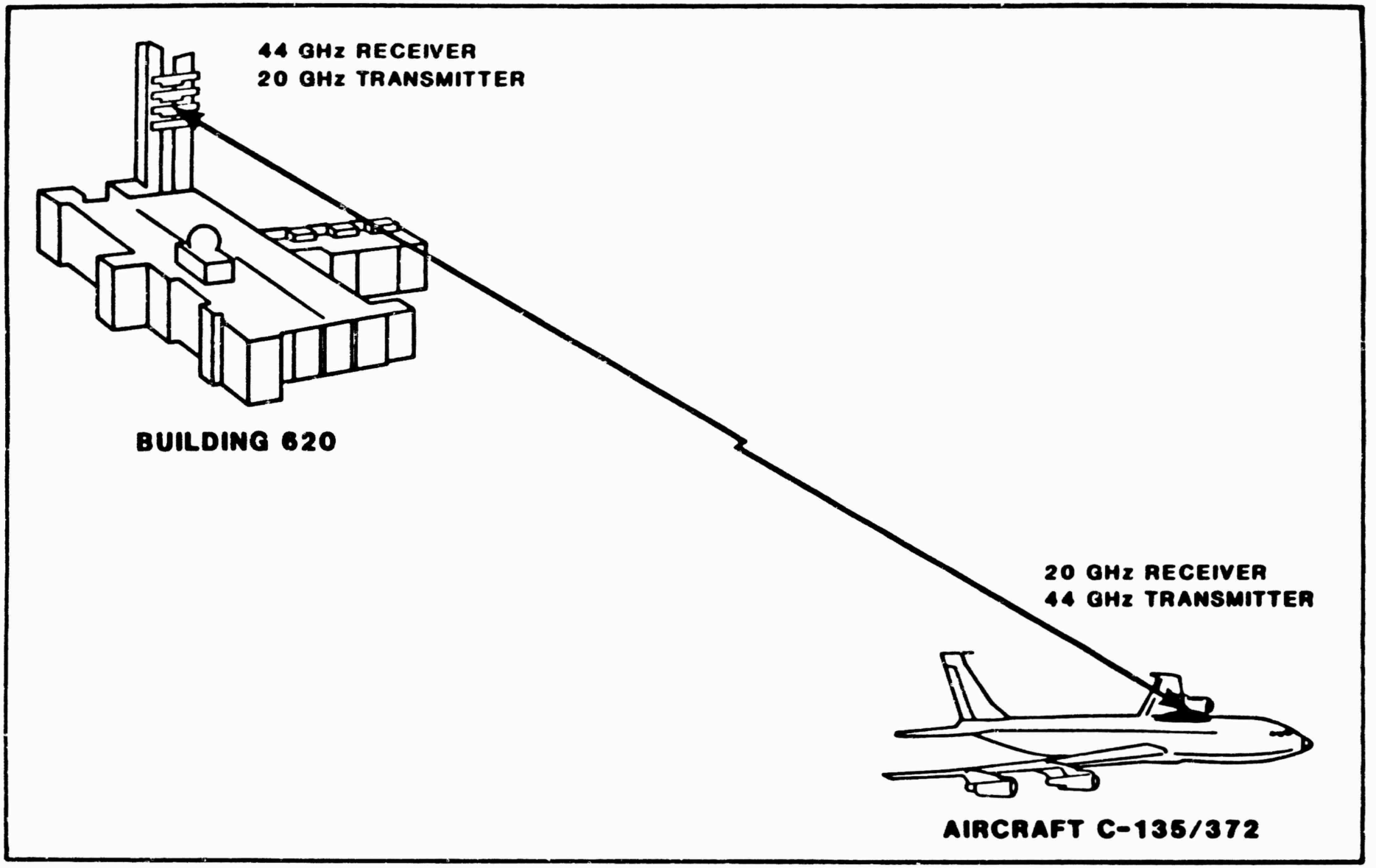

Figure 1 TRI-BAND RADOME BEAM SQUINT TEST CONFIGURATION

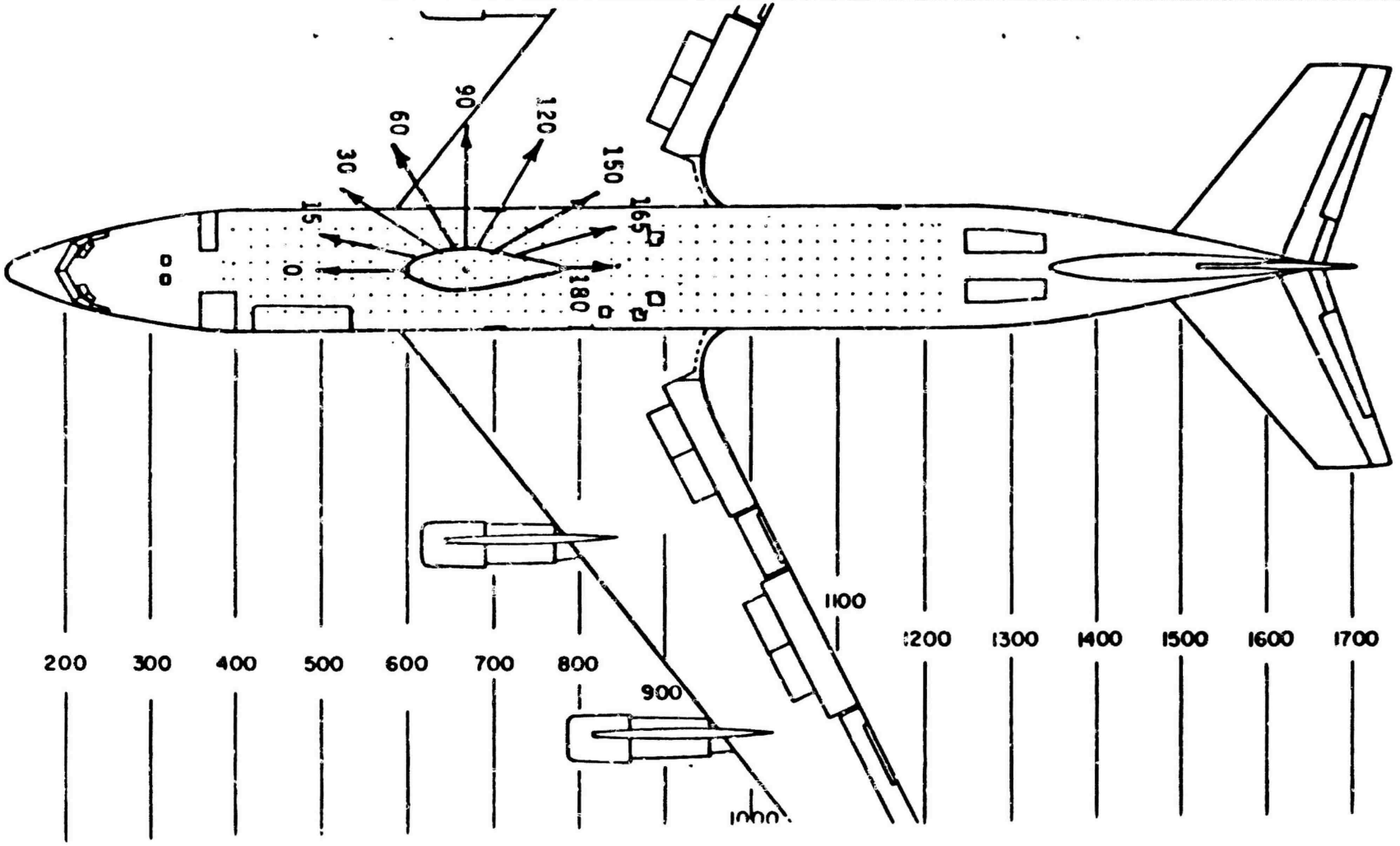

FIGURE 2 ANGLES FOR BEAM SQUINT TEST MEASUREMENTS

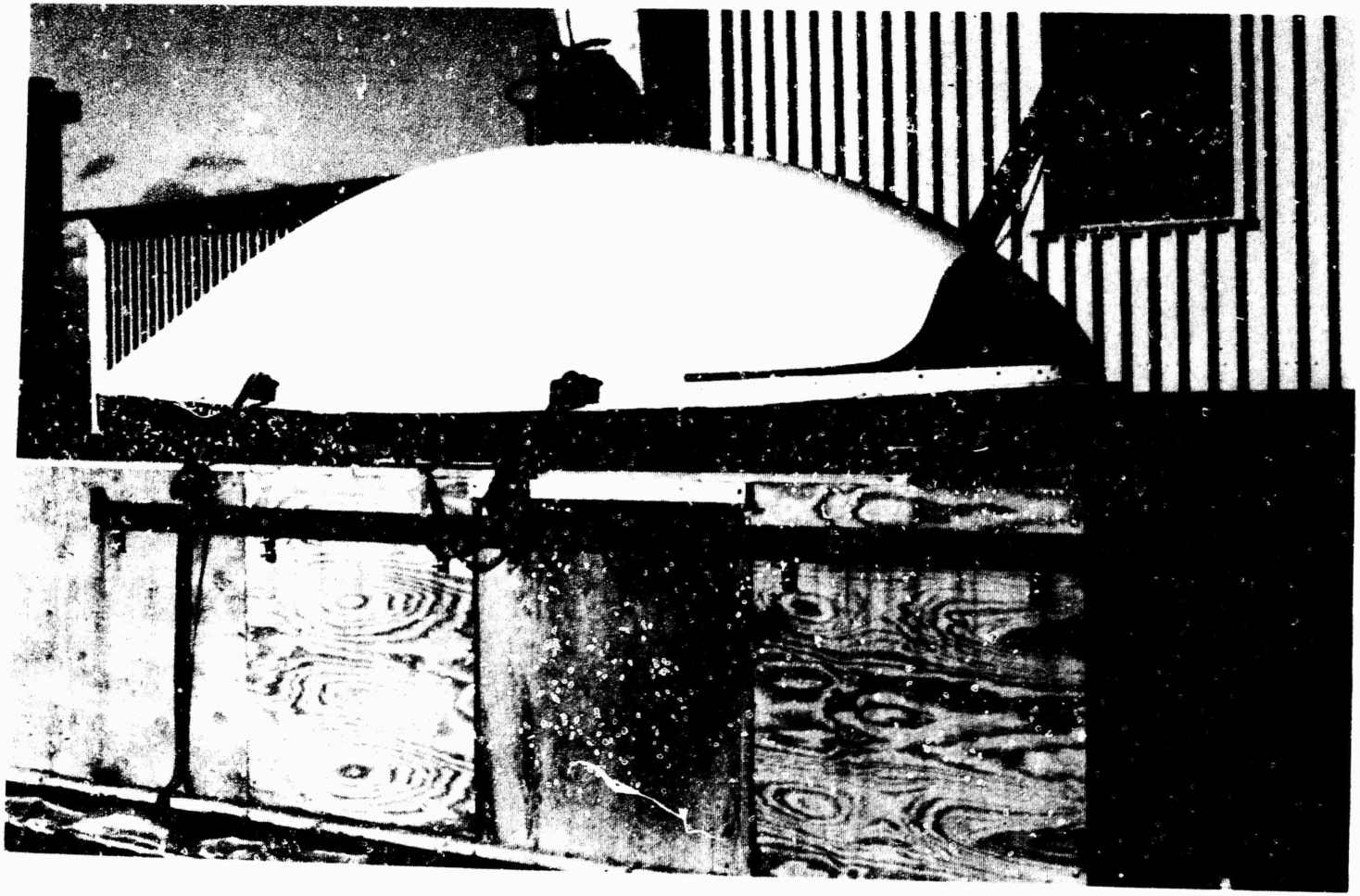

FIGURE 3 ANTENNA/RADOME TEST FIXTURE FOR TEMPERATURE & RFI TEST

FIGURE 4 AN/ASC-30 RADOME ON C-135 AIRCRAFT

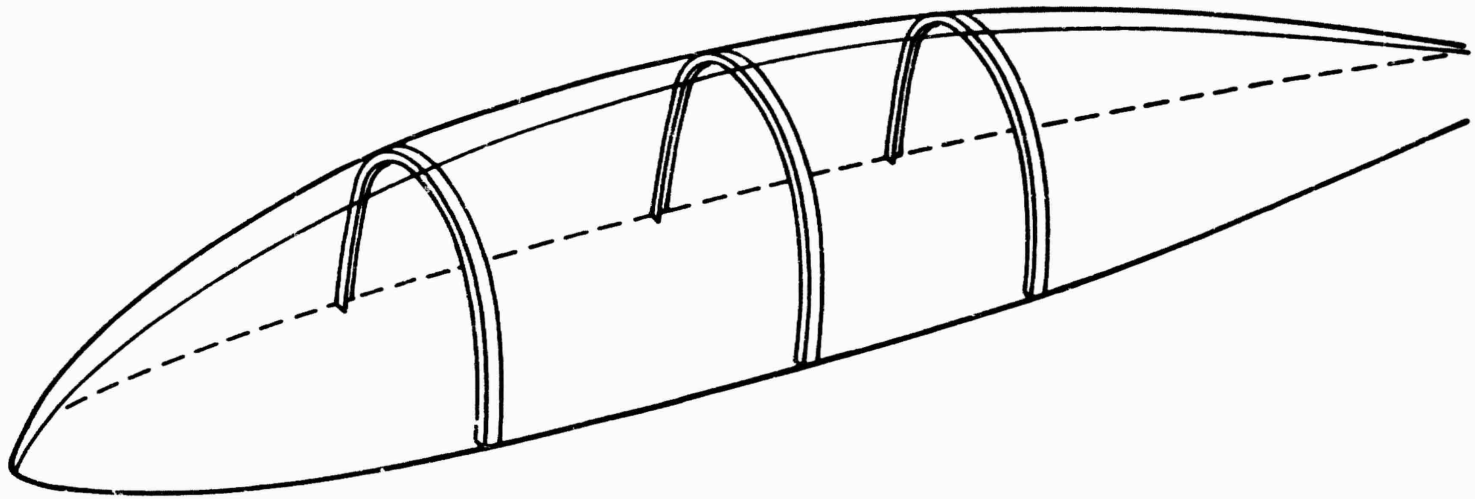

FIGURE 5 **RIB PLACEMENT FOR AFWAL TRI-BAND RADOME**

AN/ASC-30 UPGRADE
RADOME STRUCTURAL ANALYSIS
RECOMMENDED 3 RIB CONFIGURATION

- FINITE ELEMENT MODEL

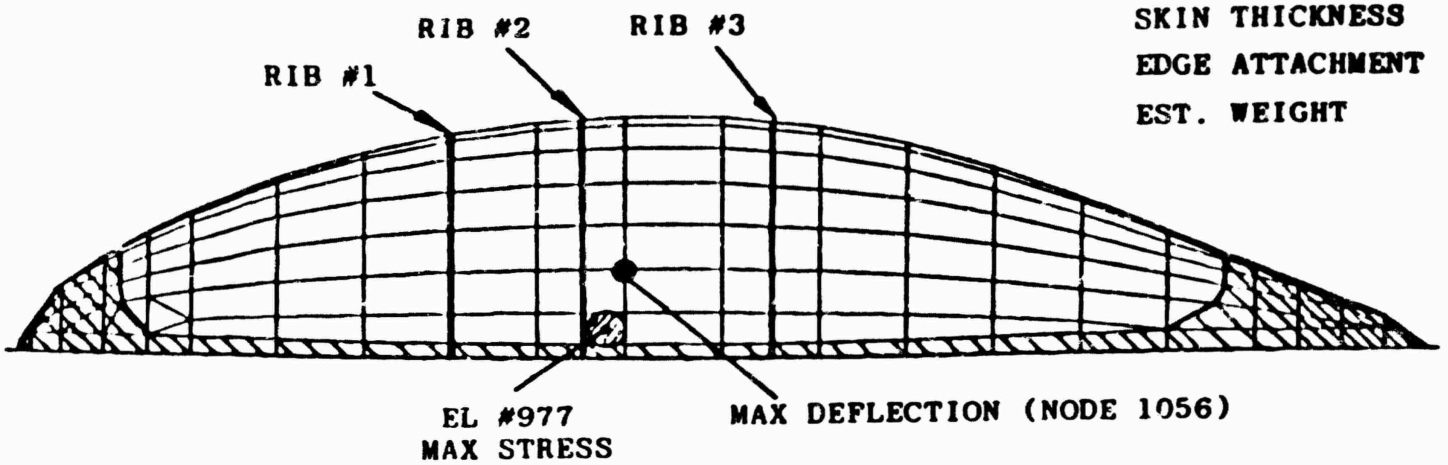

SKIN THICKNESS	0.145"
EDGE ATTACHMENT	0.290"
EST. WEIGHT	122 LBS

- RID CONSTRUCTION (KEVLAR 49 MATERIAL)

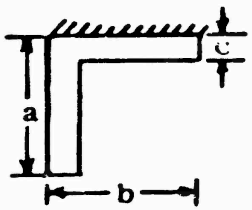

RIB TYPE	axbxc (in)
A	2x1x.145
B	2x1x.290

- MATERIAL PROPERTIES (KEVLAR 49)

$E = 4.5 \times 10^6$ PSI $\gamma = 0.2$

$G = 0.3 \times 10^6$ PSI $\delta = 0.05$ #/IN^3

Figure 6 NASTRAN FINITE ELEMENT MODEL

STRUCTURAL ANALYSIS RESULTS

- AERODYNAMIC LOAD - PER 6475-950001
- DEFLECTED MODEL

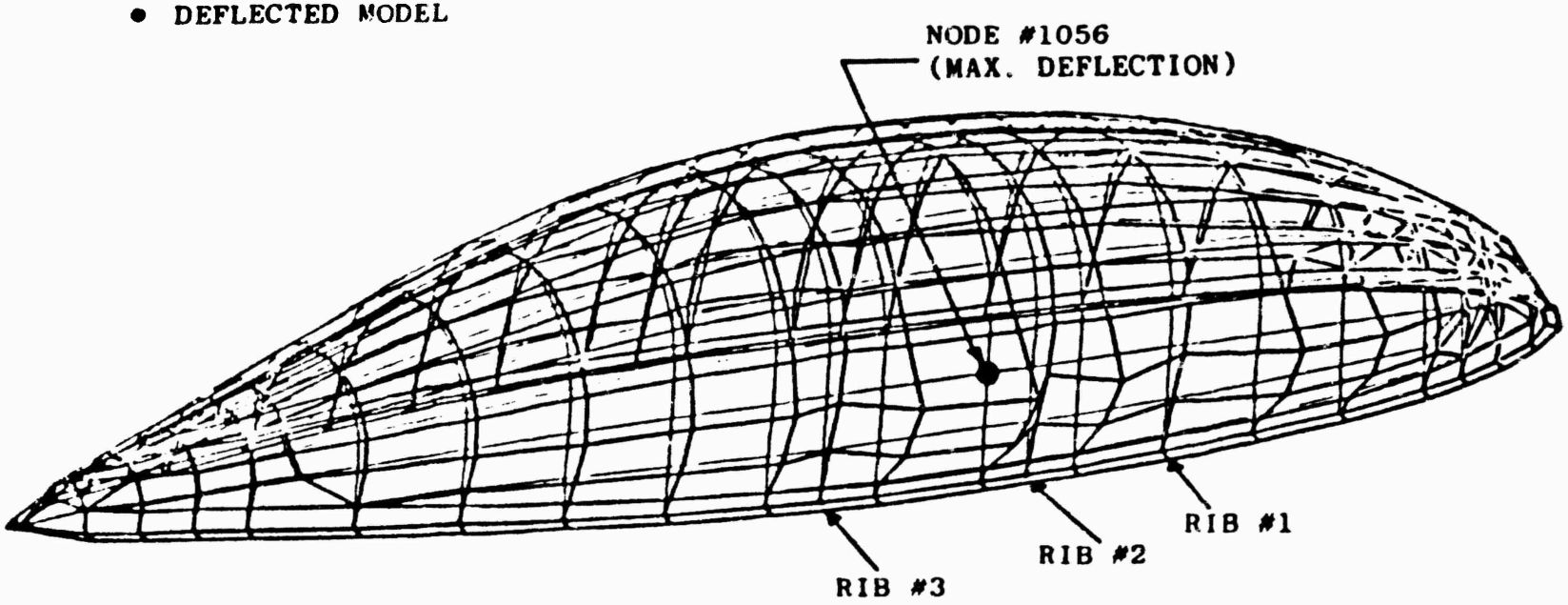

- RESULTS

CASE	RIB TYPE			MAX. DEFLEC. (IN)	MAX. STRESS (KSI)	M.S.*
	1	2	3			
I	A	A	A	.251	4.26	4.07
II	A	B	A	.238	4.23	4.10

*ALLOWABLE STRESS = 32.4 KSI, FACTORY OR SAFETY = 1.5

Figure 7 MAXIMUM DEFLECTION OF NASTRAN MODEL

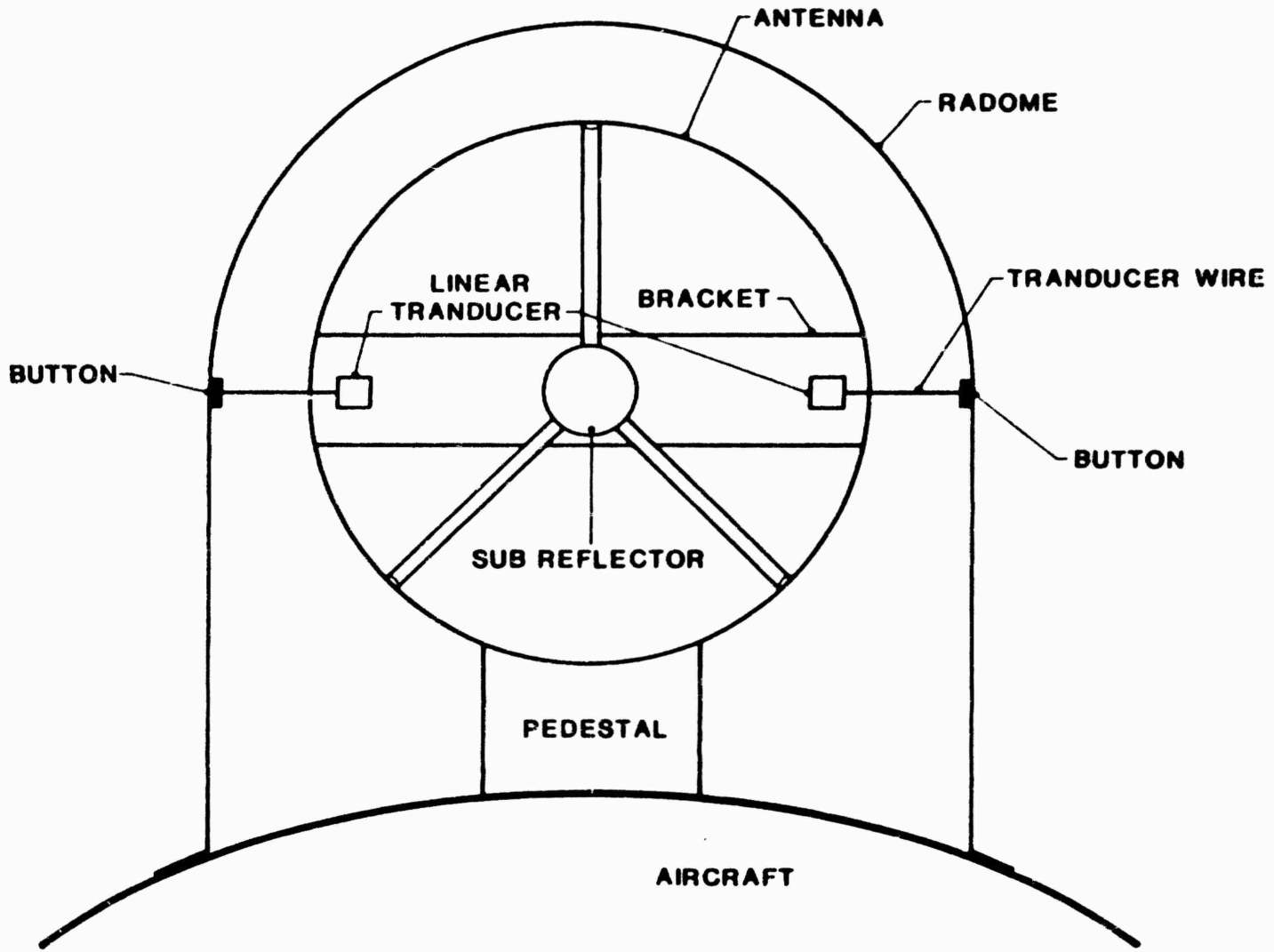

Figure 8 PHYSICAL ARRANGEMENT FOR MEASUREMENT OF RADOME DEFLECTION

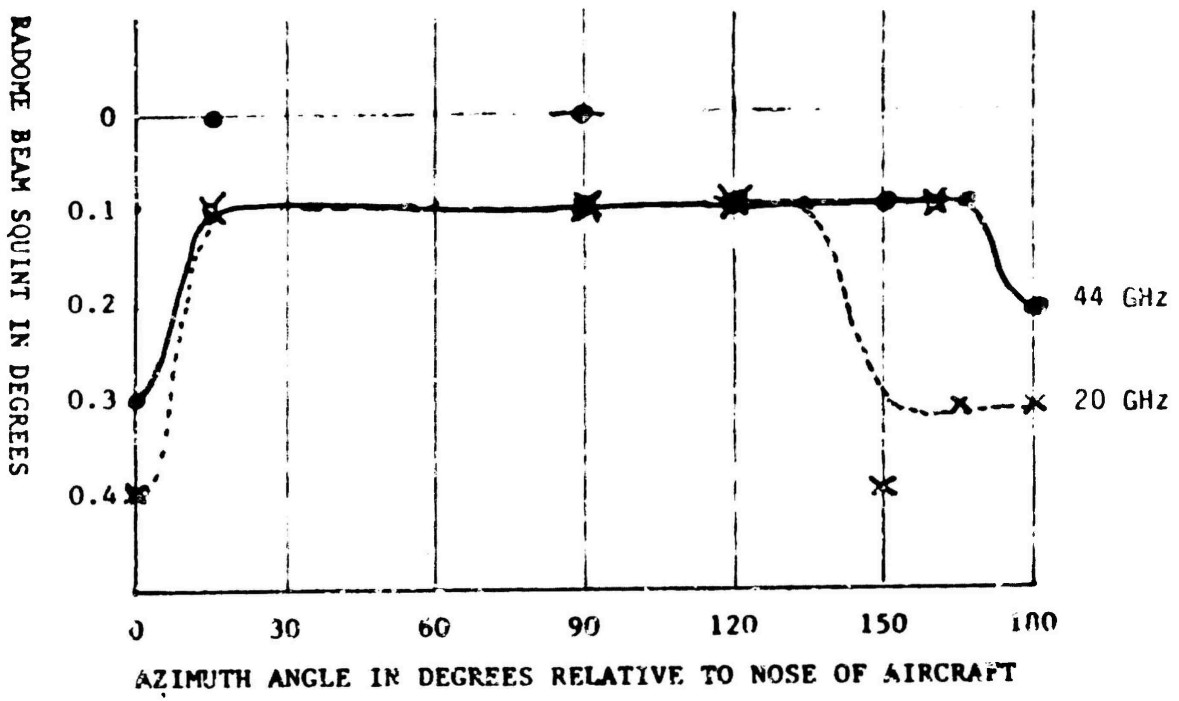

FIGURE 9 TRI-BAND RADOME BEAM SQUINT VERSUS AZIMUTH ANGLE

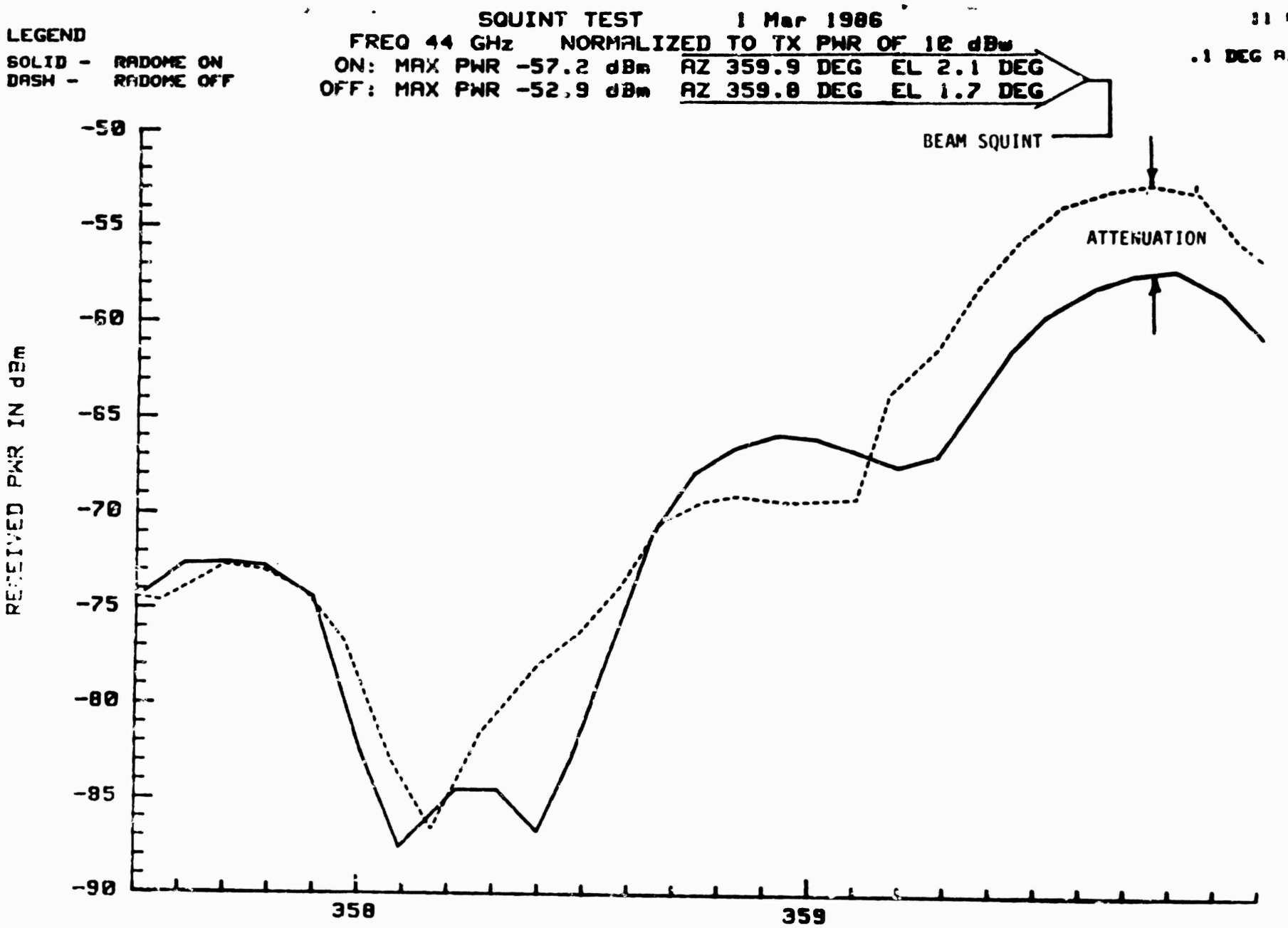

FIGURE 10 AN/ASC-30 RADOME PERFORMANCE DURING AZIMUTH SWEEP

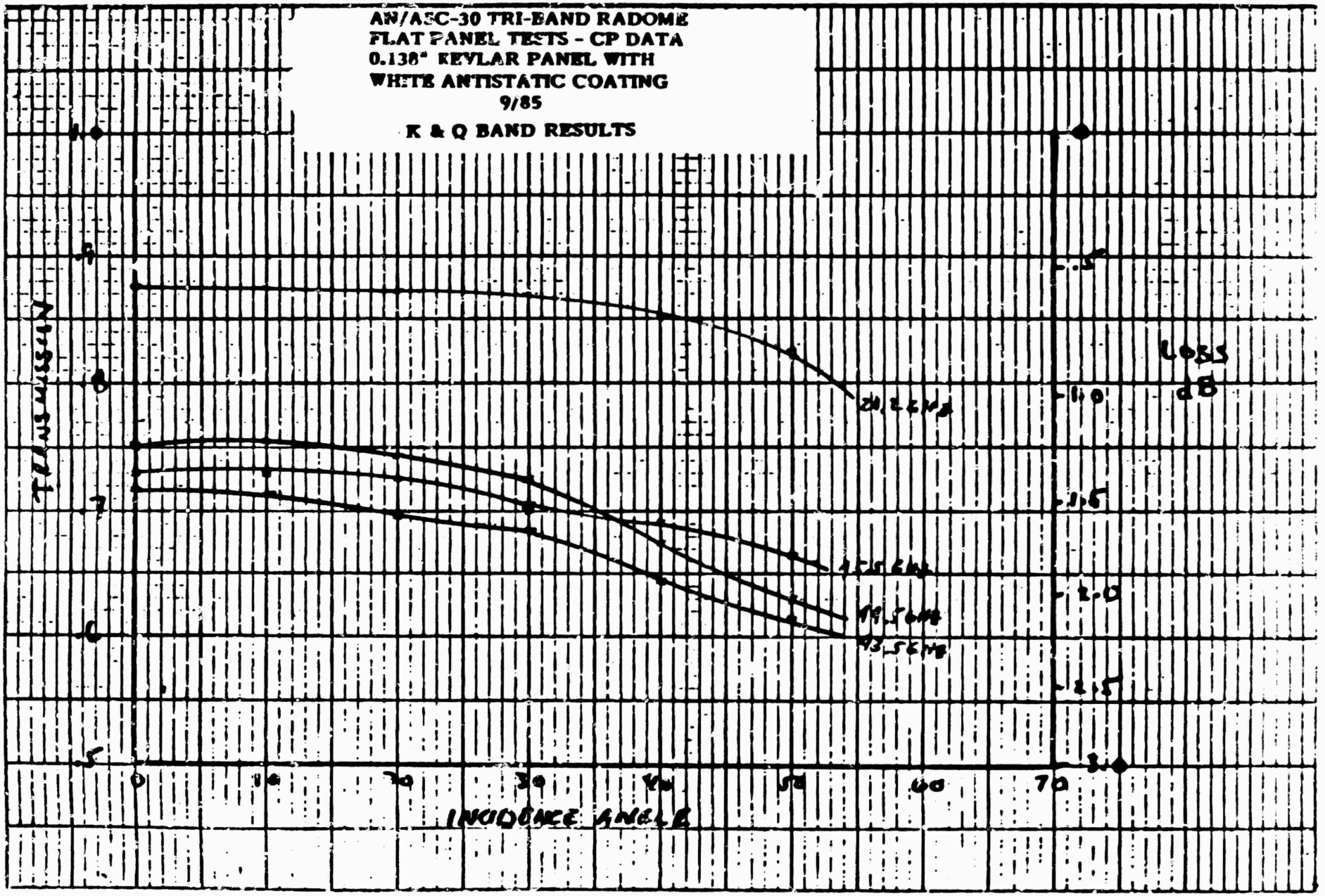

FIGURE 11 20/44 GHz FLAT PANEL MEASUREMENTS WITH COATING

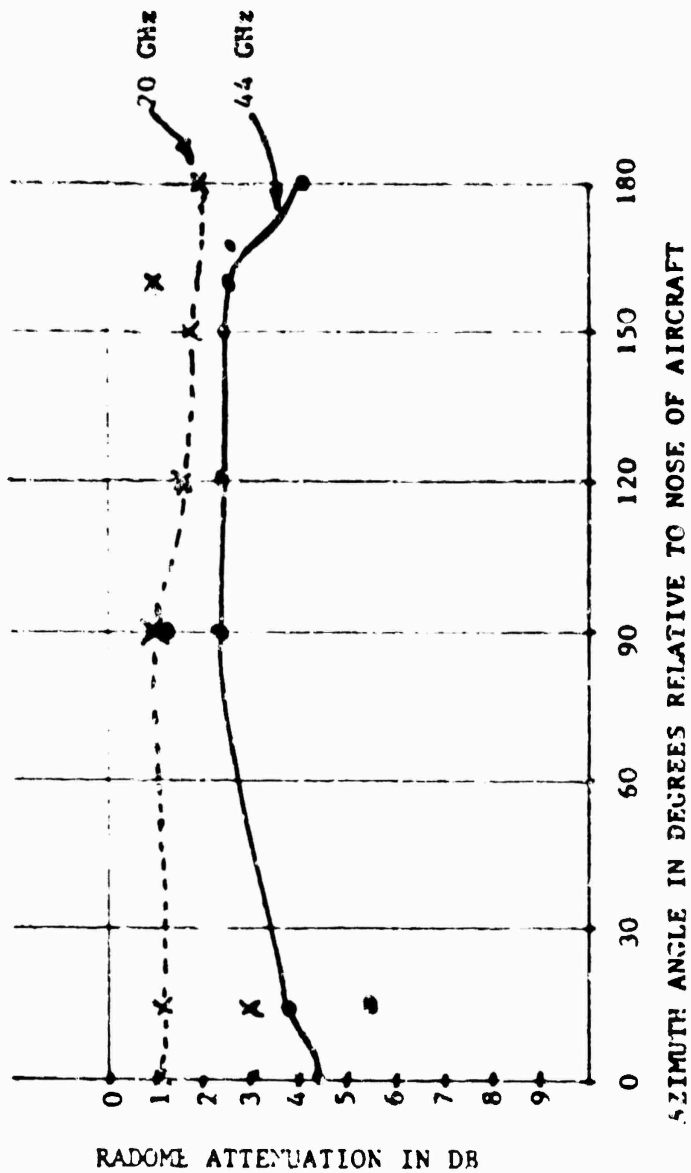

FIGURE 12 TRI-BAND RADOME ATTENUATION VERSUS AZIMUTH ANGLE

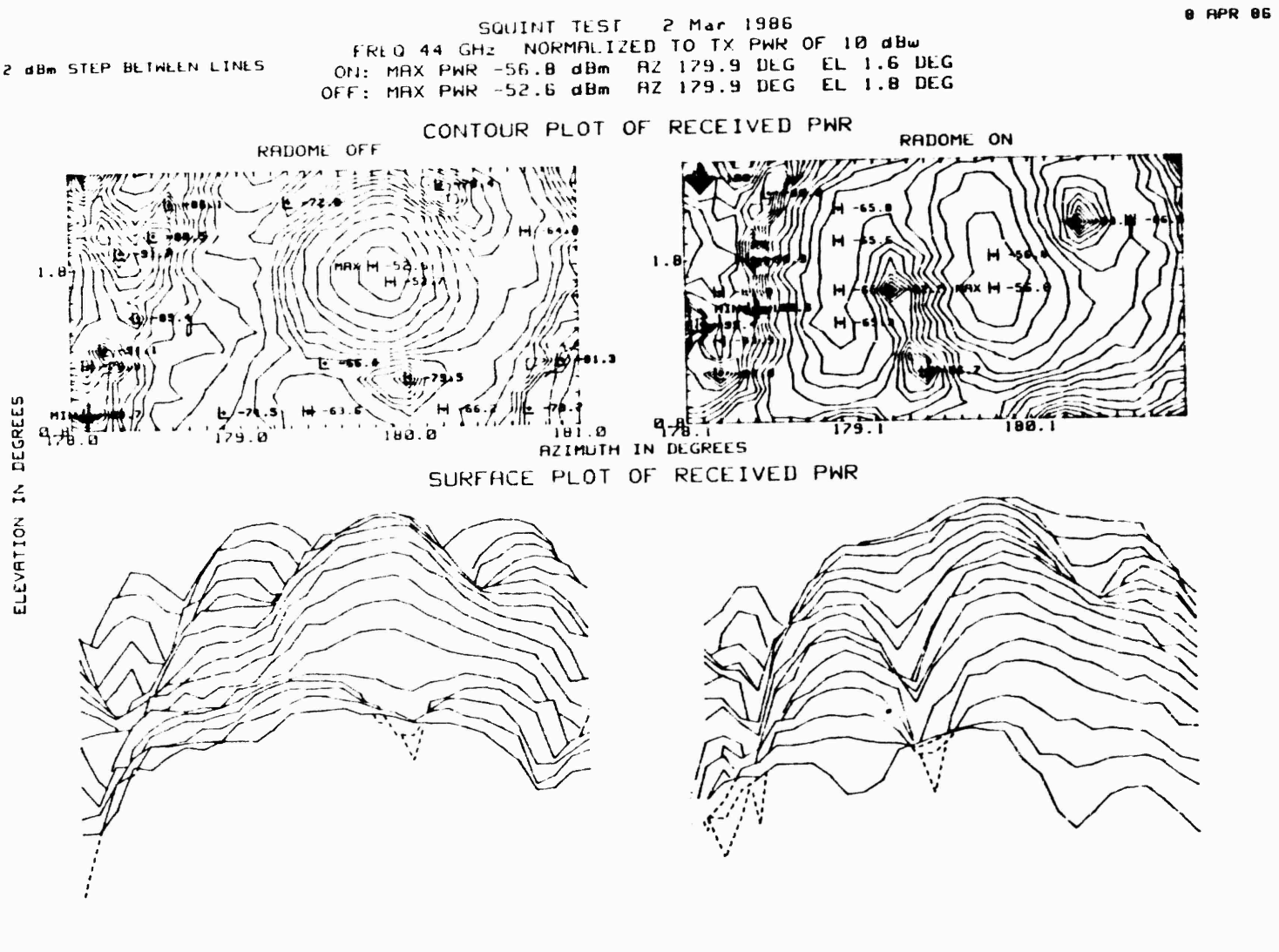

FIGURE 13 RECEIVED SIGNAL LEVEL CONTOUR PLOTS

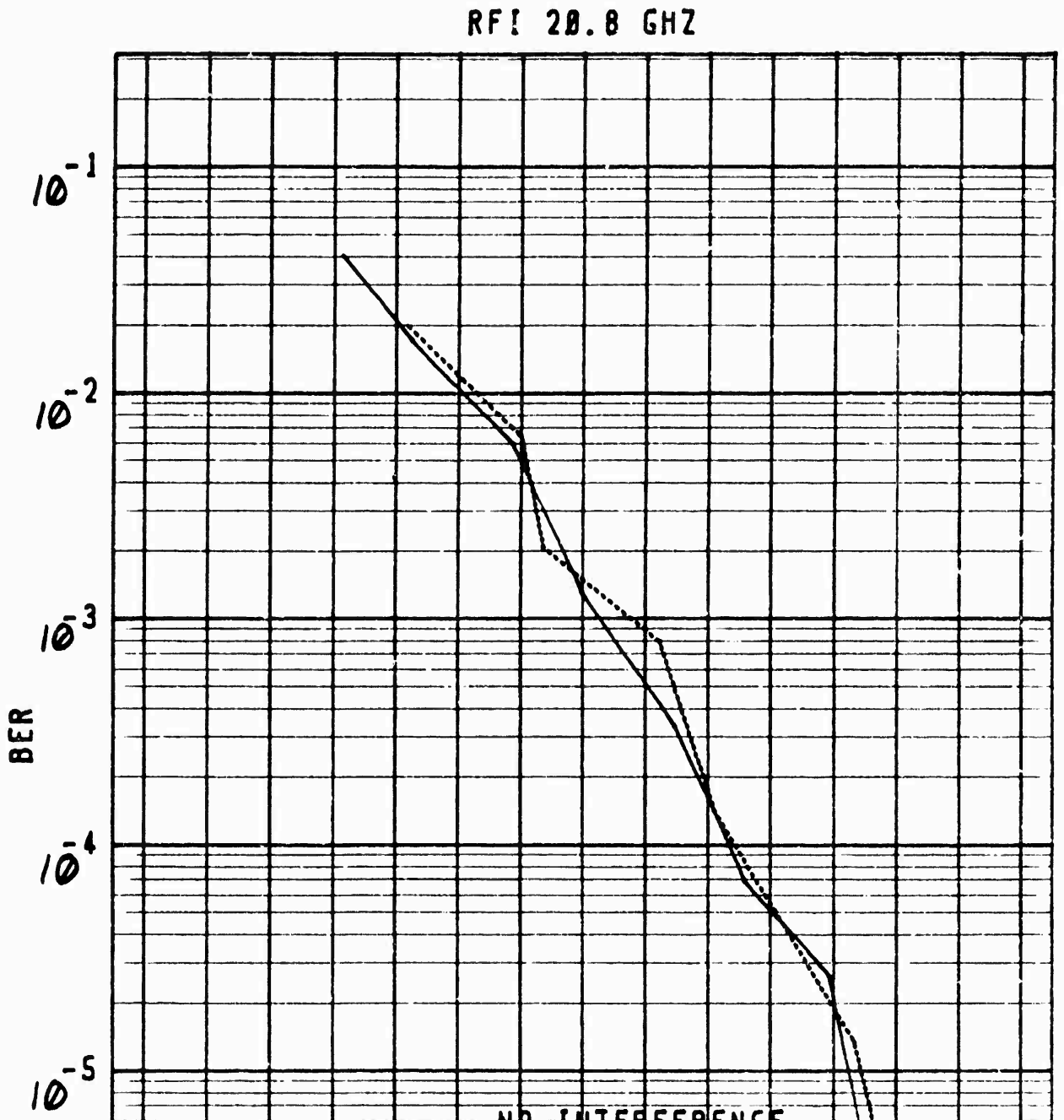

Figure 14 Bit-Error-Rate During Interference Test

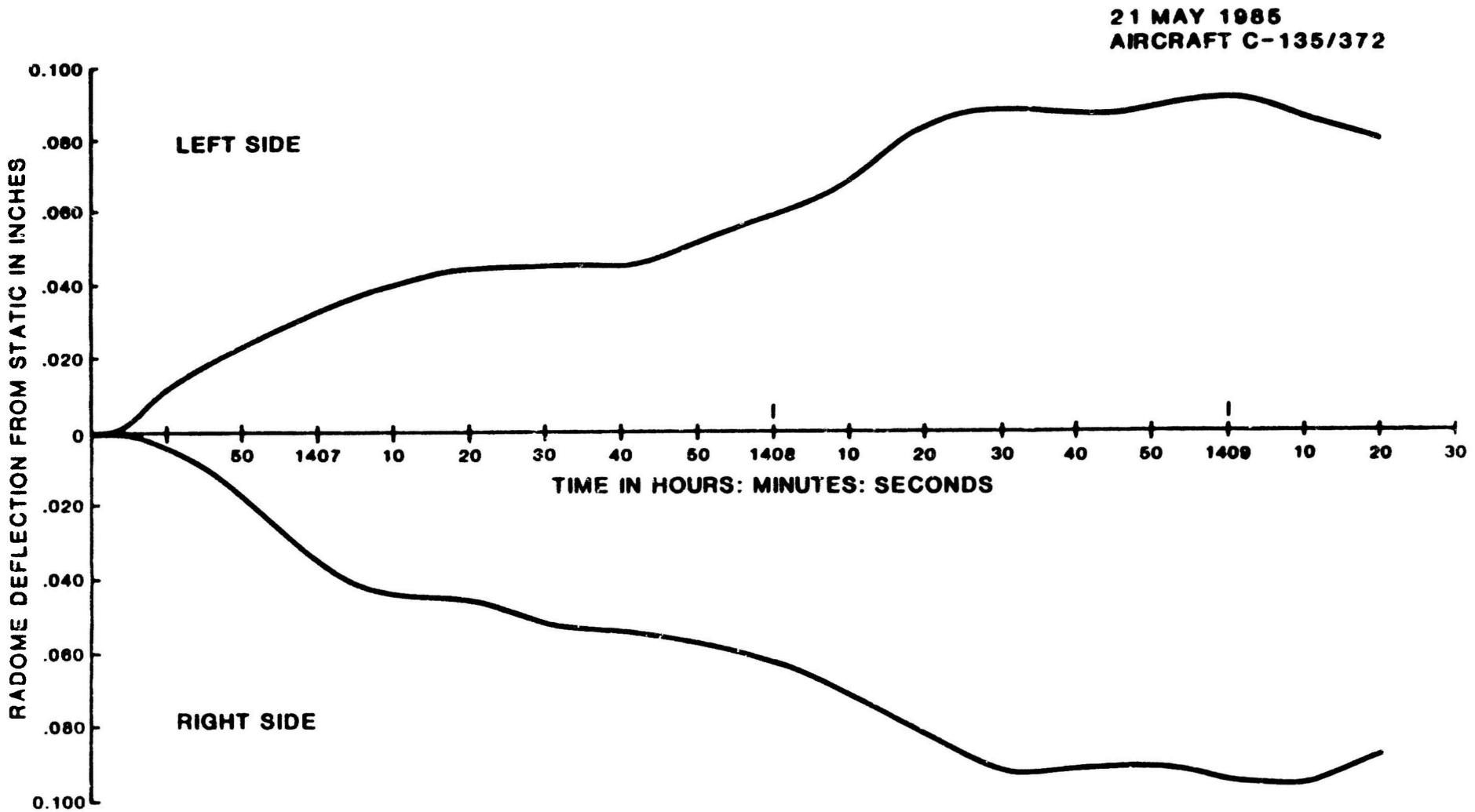

Figure 15 DEFLECTION OF TRI-BAND RADOME DURING TAKE-OFF ROLL

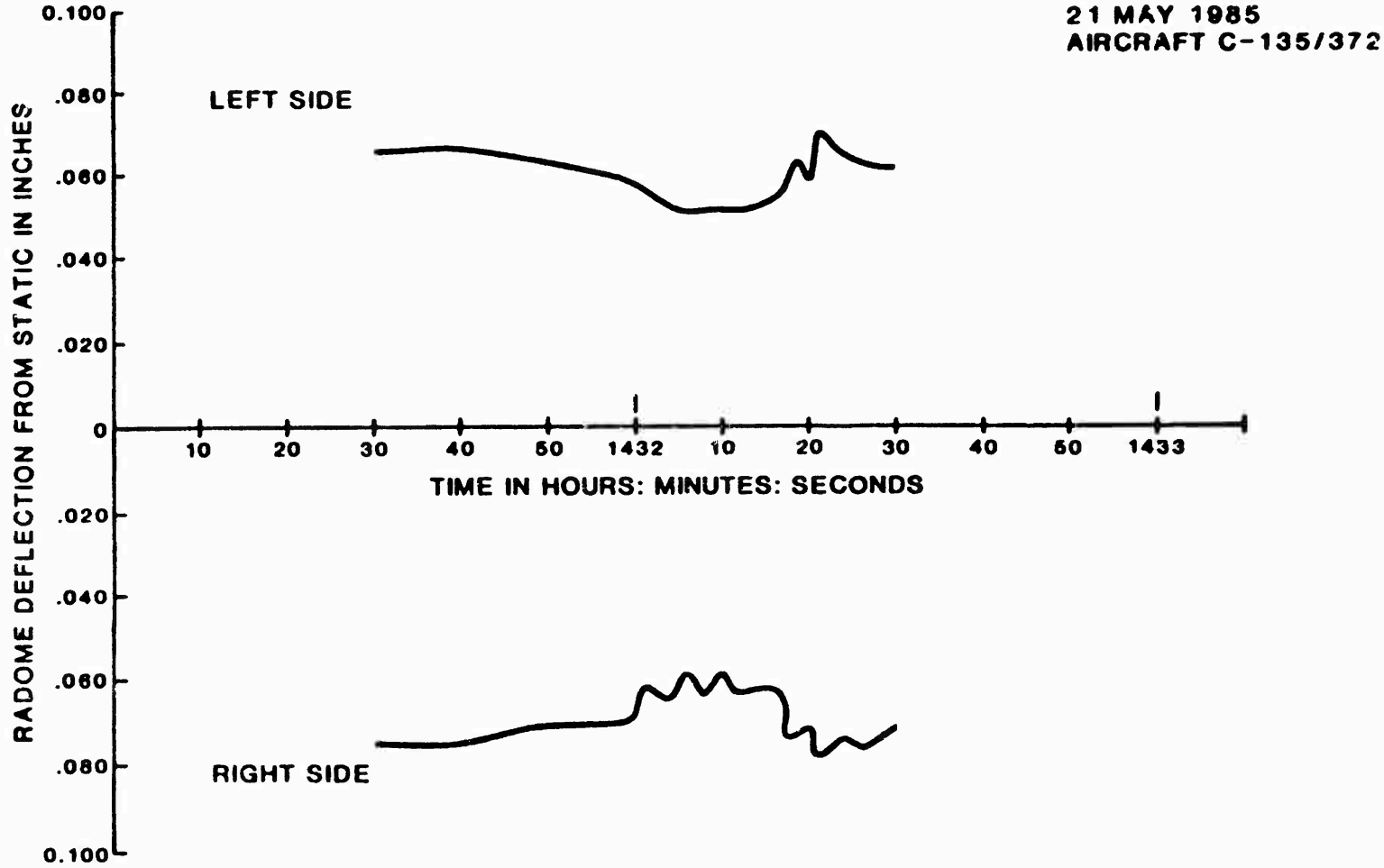

Figure 16 **DEFLECTION OF TRI-BAND RADOME DURING 8° LEFT SIDE SLIP**

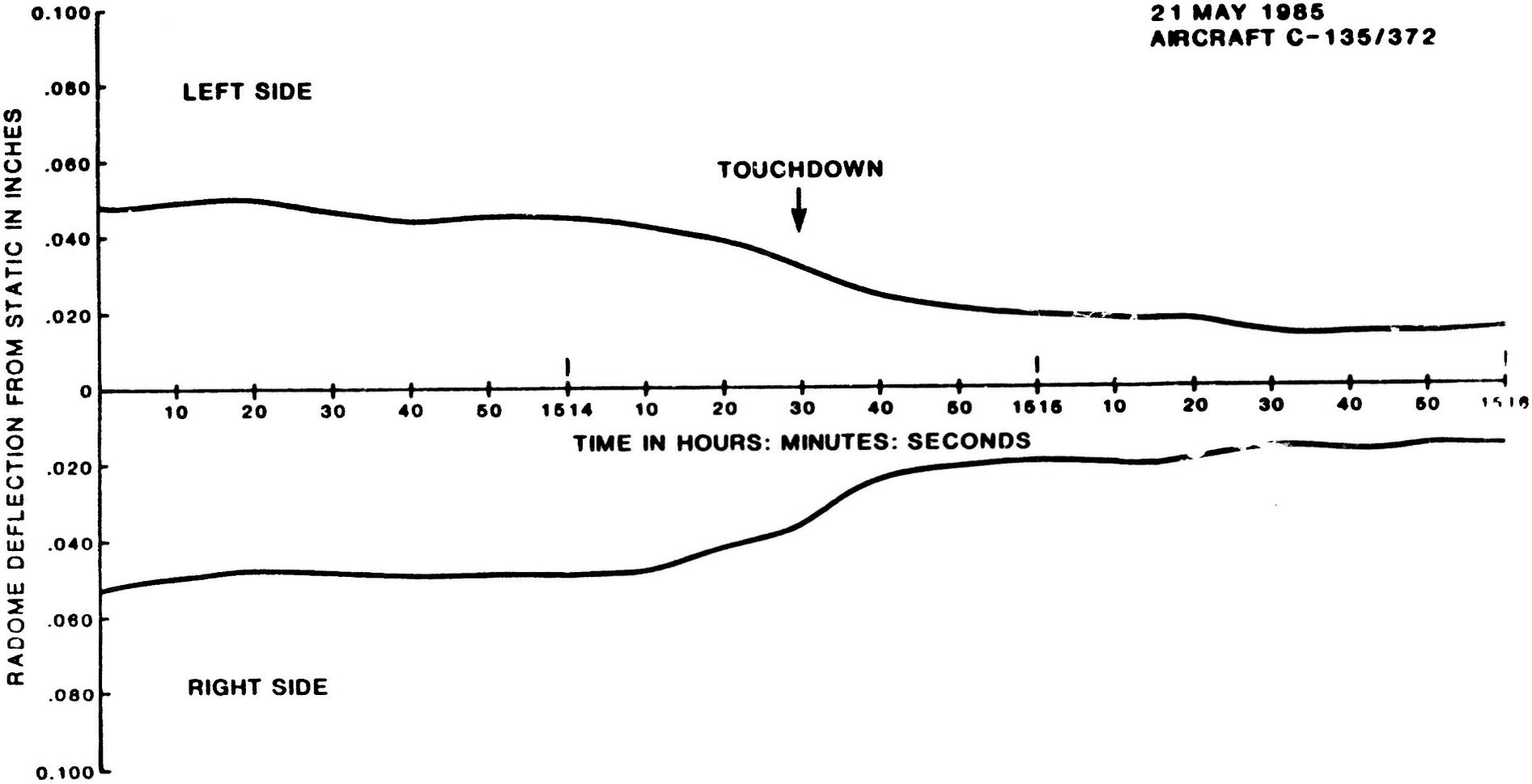

Figure 17 DEFLECTION OF TRI-BAND RADOME DURING LANDING